

intermediate position between n_{A^+} and n_{A^-} levels, and the π_{3+} level becomes more stable than the nearly degenerate π_{2-} and π_{2+} MO's.

Finally, we point out that in this simple model the splitting and the barycenter destabilization for each pair of MO's are dominated by the contributions of C_{ir} atoms (1-2 interactions), because already for 1-3 interactions the overlap (and hence the coupling) becomes an order of magnitude lower. The main exception is found for the n levels of (I): due to the strong localization of these orbitals on nitrogen atoms, 1-4 interactions between lone pairs are of the same order of magnitude as the 1-2 interactions between C_{ir} atoms. However, 1-3 interactions between C_{ir} and N atoms are antibonding (Scheme I) and nearly compensate (there are two 1-3 interactions for each 1-4 interaction) the direct coupling between lone pairs; as a consequence, even in this case, the splitting is determined by the C_{ir} atoms.

On this basis we can gain better insight into the splittings between n_{A^+} and n_{A^-} levels in the whole series of molecules. In fact, the coefficients of C2 and C5 atoms (which become C_{ir} atoms in I and IV, respectively) are similar in the n_A level of pyrimidine and much higher than the coefficient of the C4 atom (which becomes C_{ir} in II and III). As a consequence, we expect

$$\Delta E(I) \simeq \Delta E(IV) > \Delta E(II) \simeq \Delta E(III)$$

in perfect agreement with experimental findings.

Analogous considerations explain the behavior of π_2 orbitals: they are nearly degenerate in I and IV because the participation of C_{ir} AO's is symmetry forbidden. The partial breakdown of symmetry constraints in II and III allows a contribution of C_{ir} atoms to these orbitals; it results in a significant splitting. Finally, in the π_3 orbital of pyrimidine, the coefficient of the C5 atom is larger than the coefficient of the C2 atom (Table I); as a consequence, the splitting between π_{3+} and π_{3-} levels is larger in IV than in I.

Concluding Remarks

From an experimental point of view, the relevant differences among spectral patterns of the four examined compounds, despite their structural similarity, point out large differences in the interactions between the two pyrimidine rings. In this frame, the HAM/3 method has been proven to be the most successful in

reproducing quantitatively absolute energy values and relative ordering of ionic states. Ab initio STO-3G computations can be profitably used to analyze the origin of trends and relative spacings (within the two groups of n and π orbitals) with reference to the pyrimidine fragment.

An analysis of the relative importance of the various effects in determining the relative ordering and splitting of ionic states has been performed also. It shows that 1-3 and 1-4 interactions are negligible or nearly compensate each other, so that the most relevant role is always played by the direct coupling between AO's of C_{ir} atoms and/or by the percentage of nitrogen AO's (due to their higher electronegativity).

On this basis, a simple interpretative model that leads to the following rules of thumb has been proposed: (1) The bigger the coefficients of atomic orbitals of C_{ir} are the larger is the splitting between a pair of levels (deriving from the same level of pyrimidine). (2) The barycenter of a pair of related orbitals is always destabilized with respect to the corresponding ionization energy of pyrimidine due to four-electron two-level interactions. (3) Due to electrostatic repulsion, vicinal dispositions of nitrogen lone pairs destabilize the resulting MO's.

The only effect that cannot be reproduced by the proposed model is the dissymmetry between MO's belonging to the same pair, which gives the last rule: (4) The higher the contribution of more electronegative atoms is, the larger the stabilization of the corresponding MO.

In conclusion, we think that a careful analysis of the interactions present in a related class of molecules may provide a valuable aid in the interpretation of PE spectra of large molecules in which first-principle computations are hardly feasible. Simple models based on well-chosen fragments and supported by HAM/3 computations seem particularly adequate in this connection.

Acknowledgment. We acknowledge Professor E. Lindholm for his useful comments and careful reading of the manuscript, Professor T. Kauffmann for the generous gift of samples of the different bipyrimidines, and Dr. L. Asbrink for providing a copy of the HAM/3 program.

Registry No. I, 34671-83-5; II, 2426-94-0; III, 28648-89-7; IV, 56598-46-0; pyrimidine, 289-95-2.

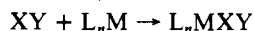
Oxidative Addition of Hydrogen to Bis(phosphine)platinum(0) Complexes: An ab Initio Theoretical Treatment

J. Oakey Noell[†] and P. Jeffrey Hay*

Contribution from the Theoretical Division, Los Alamos National Laboratory, University of California, Los Alamos, New Mexico 87545. Received June 8, 1981

Abstract: Ab initio molecular orbital methods utilizing relativistic core potentials and correlated wave functions are employed to examine the oxidative addition reactions $H_2 + Pt(PH_3)_2 \rightarrow cis-Pt(PH_3)_2H_2$ and $H_2 + Pt[P(CH_3)_3]_2 \rightarrow cis-Pt[P(CH_3)_3]_2H_2$. For this symmetry-allowed process, an activation barrier of 17 kcal/mol and an exothermicity of 7 kcal/mol are calculated at the SCF level for the PH_3 liquid; similar values are obtained for the $P(CH_3)_3$ ligand. This implies a barrier of 24 kcal/mol for the reverse reductive elimination reaction. These values were not significantly altered in MC-SCF or CI calculations. This barrier is consistent with available data on the analogous process in six-coordinate complexes but is puzzling in light of the paucity of known four-coordinate cis dihydrides. The reaction is analyzed in terms of three phases: initial repulsion, partial transfer of charge from the platinum to the hydrogen, and final metal-hydrogen bond formation. The relative energies of the cis and trans isomers are also discussed.

The well-established inorganic reaction,¹⁻⁴ oxidative addition of ligands to a metal center,



has often been postulated in homogeneous catalytic cycles.⁵ From a mechanistic viewpoint, these reactions have continued to be the

subject of many studies. For additions to square-planar d^8 complexes, one generally finds concerted additions of homonuclear

(1) Collman, J. P. *Acc. Chem. Res.* 1968, 1, 136.

(2) Vaska, L. *Acc. Chem. Res.* 1968, 1, 335.

(3) Halpern, J. *Acc. Chem. Res.* 1970, 3, 386.

(4) Cotton, F. A.; Wilkinson, G. "Advanced Inorganic Chemistry", 3rd ed.; Interscience: New York, 1972; p 772.

(5) James, B. R. "Homogeneous Hydrogenation"; Wiley: New York, 1973.

[†] Present address: Division 8343, Sandia National Laboratory, Livermore, CA 94550.

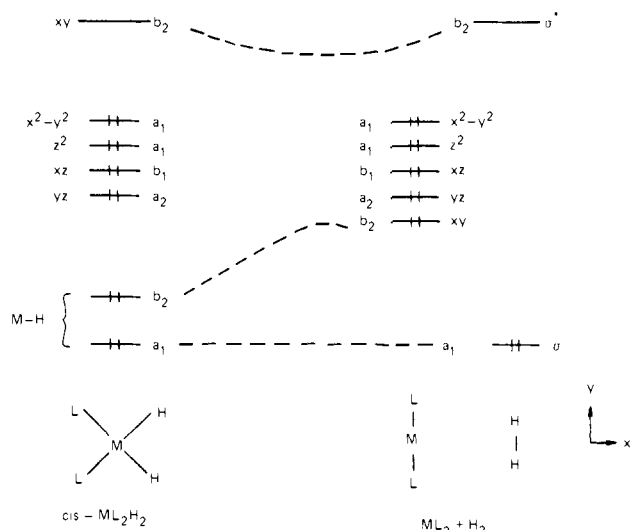
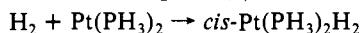


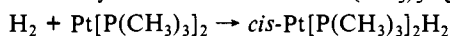
Figure 1. Orbital correlation diagram for cis addition.

diatomics to yield cis products, while one observes two-step addition of polar adducts to yield trans products.⁶⁻¹⁰ Exceptions to these rules of thumb have been noted, however.¹¹

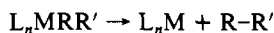
In this paper, we consider theoretically the reaction path of a model oxidative addition of H_2 to $Pt(0)$ with a model PH_3 ligand



and a limited study with a more realistic $P(CH_3)_3$ ligand



There is relatively little data regarding such additions to d^{10} metal centers, although H_2 has been observed¹² to react with PtP_2 to form $trans-Pt_2H_2$ where $P = P(i-Pr)_3$ and other trialkylphosphines. The reverse reaction of reductive elimination from a d^8 center



has been observed for $R = CH_3$, $R' = H$ from four-coordinate $Pt(II)$ phosphine complexes,¹³ for $R = R' = CH_3$ from three-coordinate $Pd(II)$ phosphine complexes,¹⁴ for $R = R' = CH_3$ from three-coordinate trialkyl gold(III) complexes¹⁵ and for tetramethylene elimination from five-coordinate nickel(II) phosphine complexes.¹⁶ One of the few examples of $Pt(0)$ oxidative addition¹⁷ involves the insertion into the strained C-C bond of cyclopropane by $(PR_3)_2Pt(C_2H_4)$ to form a platinumacyclobutane, $(PR_3)_2PtCH_2CH_2CH_2$, but it is not known whether prior dissociation of C_2H_4 occurs.

Although molecular hydrogen is a common reactant with metal centers, these reactions considered here have not been observed per se. Indeed cis dihydrides involving a d^8 metal are not commonly observed and have been isolated only with very bulky substituents on the phosphine ligands or with a bidentate phosphine ligand.^{18,19} This instability is thought to be kinetic in origin.¹⁰

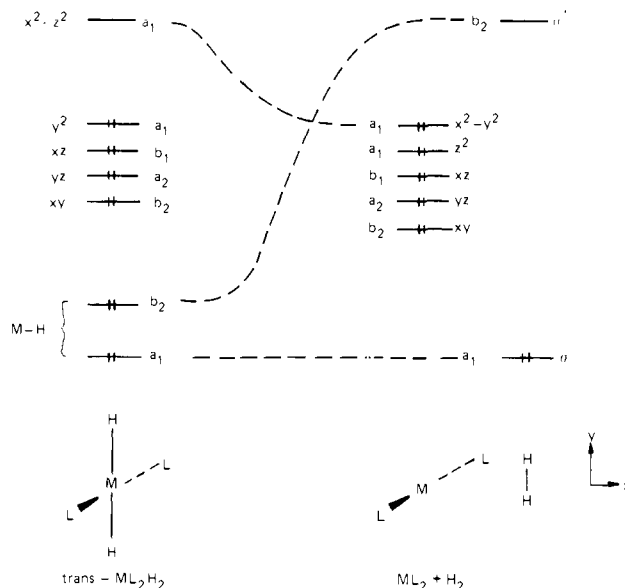


Figure 2. Orbital correlation diagram for trans addition.

It is our intent to address this question from a theoretical viewpoint by following the minimum energy path as the hydrogen undergoes addition to the complex. Preliminary accounts of this work have been given previously.²⁰ Also, practically all theoretical treatments²¹ of phosphine ligands to date have employed the model PH_3 ligand, whereas the simplest phosphine ligand to have a coordination chemistry is the $P(CH_3)_3$ moiety (also referred to as PMe_3 here). We also investigate in this study the differences between these two ligands in platinum dihydride complexes. These calculations, which are among the few studies to date of an oxidative addition to a transition-metal species, thus represent the first ab initio study to our knowledge of a realistic phosphine complex.

General Considerations

The addition of hydrogen to form the cis isomer of $PtH_2(PH_3)_2$ is a symmetry-allowed process,²²⁻²⁵ as shown by the orbital correlation diagram in Figure 1. The $Pt-H$ bonding orbitals in the complex of a_1 and b_2 symmetry correlate with the H_2 bonding orbital (a_1) and $Pt 5d_{xy}$ orbital (b_2) of the products. This situation is contrasted by the symmetry-forbidden process leading to the trans isomer (Figure 2). There one expects a barrier due to the formal change in symmetry of the occupied orbitals, since the $Pt-H$ orbitals (again a_1 and b_2) do not correlate with the $H_2 \sigma$ and $5d_{xz-yz}$ orbitals (both a_1). This difference between the cis and trans isomers has been used to explain the presumed kinetic instability of the cis isomer and to rationalize the usual observance of only trans isomers.¹⁸

The fact that the concerted pathway of reductive elimination from the cis isomer is symmetry allowed does not necessarily imply the lack of an appreciable barrier. As an example, the trimerization of acetylene to form benzene has no barriers imposed by symmetry but nonetheless has a high barrier as the alkyne character is retained far along the reaction coordinate before aromatic stabilization sets in.²⁶ Symmetry arguments do not even

(6) Chock, P. B.; Halpern, J. *J. Am. Chem. Soc.* **1966**, *88*, 3511.

(7) Ugo, R.; Pasini, A.; Fusi, A.; Cenini, S. *J. Am. Chem. Soc.* **1972**, *94*, 7364.

(8) Kubota, M.; Kiefer, G. W.; Ishikawa, R. M.; Bencala, K. E. *Inorg. Chim. Acta* **1973**, *7*, 195.

(9) Burgess, J.; Hacker, N. J.; Kemmitt, R. D. W. *J. Organomet. Chem.* **1974**, *72*, 121.

(10) Meurelnik, R. J.; Weitzberg, M. Blum, J. *Inorg. Chem.* **1979**, *18*, 915.

(11) Harrod, J. F.; Hamer, G.; Yorke, W. J. *Am. Chem. Soc.* **1979**, *79*, 3987.

(12) Yoshida, T.; Otsuka, S. *J. Am. Chem. Soc.* **1977**, *99*, 2134.

(13) Abis, L.; Sen, A.; Halpern, J. *J. Am. Chem. Soc.* **1978**, *100*, 2915.

(14) Milstein, D.; Stille, J. K. *J. Am. Chem. Soc.* **1979**, *101*, 4981. Gillie, A.; Stille, J. K. *Ibid.* **1980**, *102*, 4933.

(15) Kamiya, S.; Albright, T. A.; Koch, J. J. *Am. Chem. Soc.* **1976**, *98*, 7255; **1977**, *99*, 8840.

(16) Grubbs, R. H.; Miyashita, J. *Am. Chem. Soc.* **1978**, *100*, 1300.

(17) Lenarda, M.; Ros, R.; Graziani, M.; Belluco, U. *J. Organomet. Chem.* **1974**, *70*, 133. Rajaram, J.; Ibers, J. A. *J. Am. Chem. Soc.* **1978**, *100*, 829.

(18) Yoshida, T.; Yamagata, T.; Tulip, T. H.; Ibers, J. A.; Otsuka, S. *J. Am. Chem. Soc.* **1978**, *100*, 2063 and references therein.

(19) Moulton, C. J.; Shaw, B. L. *J. Chem. Soc., Chem. Commun.* **1976**, 365.

(20) Preliminary results of these calculations have been presented: (a) Hay, P. J., "Abstracts of Papers", 179th National Meeting of the American Chemical Society, Houston, TX, March 23-28, 1980; American Chemical Society: Washington D.C., 1980; INOR. (b) Hay, P. J., Seventh Canadian Symposium on Theoretical Chemistry, Banff, Canada, June 15-20, 1980.

(21) Examples of PH_3 ligands in ab initio calculations: (a) Dedieu, A. *Inorg. Chem.* **1980**, *19*, 375. (b) Bachmann, C.; Demuyneck, J.; Veillard, A. *J. Am. Chem. Soc.* **1978**, *100*, 2366.

(22) Pearson, R. G. *Acc. Chem. Res.* **1971**, *4*, 152.

(23) Braterman, P. S.; Cross, R. J. *Chem. Soc. Rev.* **1973**, *2*, 271.

(24) Akermarck, B.; Ljungquist, A. *J. Organomet. Chem.* **1979**, *182*, 59.

(25) Tatsumi, K.; Hoffmann, R.; Yamamoto, A.; Stille, J. K., submitted for publication.

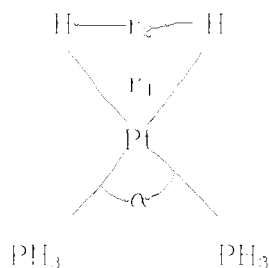
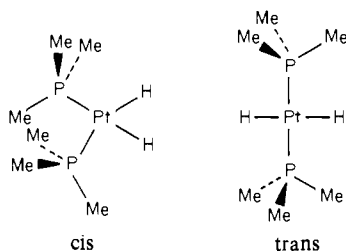


Figure 3. Optimization parameters for the C_{2v} approach of H_2 to $Pt(PH_3)_2$.

Chart I



foreclose the possibility of a nonconcerted mechanism. The Diels–Alder addition of ethylene to butadiene, a classic symmetry-allowed reaction, has been the subject of a recent controversy as to whether the reaction is concerted or passes through an asymmetric free radical state.²⁷

We were thus led to consider our model reaction, despite its possible limitations, as a means of going beyond symmetry arguments and obtaining a more rigorous theoretical description of this important class of reactions.

Computational Details

Basis Sets and Potentials. The calculations reported here employed a flexible Gaussian basis set to describe the valence electrons, while the core electrons of P and Pt were replaced by effective core potentials. The details of the basis set and potentials have been given elsewhere.²⁸ The number of primitive and contracted functions used here on the respective atoms in $Pt(PH_3)_2H_2$ are as follows: P, (3s4p) \rightarrow [2s2p]; Pt, (4s4p5d) \rightarrow [3s2p2d]; H, (5s) \rightarrow [3s] in H_2 , and (4s) \rightarrow [2s] in PH_3 . In the case of the $P(CH_3)_3$ ligand, a minimal basis (STO-3G) was employed on the C and H atoms.²⁹

Geometries. The reaction path for the concerted reaction was defined in terms of the geometric parameters in Figure 3. The parameters R_2 and α were optimized for each value of R_1 along the path. Throughout this process the platinum–phosphine bond length was fixed at 2.268 Å (see the earlier paper²⁸ for a discussion of Pt–P bond lengths). Tetrahedral bond angles were also assumed in the model PH_3 ligand.

Since the results of the $H_2 + Pt(PH_3)_2$ study showed relatively little effect in going from SCF to CI calculations, the calculations on the computationally more demanding species involving PMe_3 were carried out at the SCF (Hartree–Fock) level. For the PMe_3 ligand, the P–Pt–P and H–Pt–H angles and the Pt–H bond lengths of the complexes, transition state, and reactants were assumed without further optimization at the values calculated for the $H_2 + Pt(PH_3)_2$ reaction. The assumed orientation of the methyl groups is shown in Chart I. The CH_3 groups are all staggered with respect to the other tetrahedral bonds about P atoms. The values for Pt–P (2.247 Å) and P–C (1.83 Å) distances and C–P–C bond angles (113°) were taken from averaging the structural parameters of the related complex $cis\text{-}Pt[P(CH_3)_3]_2Cl_2$ determined

by X-ray diffraction studies of the crystal.³⁰

MC-SCF and CI Calculations. For the $Pt(PH_3)_2 + H_2$ reaction, multiconfiguration SCF (MC-SCF) and configuration interaction calculations were also carried out to examine the role of electron correlation in the reaction. If we focus on the Pt–H bonding orbitals (which, as noted above, correlated with the σ H_2 orbital and the $5d_{xy}$ Pt orbital), the primary configuration describing the complex can be written as follows:

$$\Phi_1 = \Phi_0(4b_2)^2(6a_1)^2$$

where

$$\Phi_0 = \dots (5a_1)^2(3b_2)^2(2b_1)^2(2a_2)^2$$

and $6a_1$ and $4b_2$ represent the key orbitals of interest. (The numbering at the orbitals here includes only the valence orbitals.) In addition, the configuration

$$\Phi_2 = \Phi_0(4b_2)^2(5b_2)^2$$

is needed to treat the dissociation process into $L_2Pt + H + H$, where $5b_2$ denotes the σ^* H_2 orbital at large metal–hydrogen separations. For the addition reaction itself, Φ_2 should have a significant effect for only those configurations where the H–H bond is stretched significantly. Since we did not know a priori the nature of the transition state, the reaction was treated by optimizing the orbitals and CI coefficients of the two-configuration wave function:

$$\Psi_{GVB} = C_1\Phi_1 + C_2\Phi_2$$

self-consistently by using the generalized valence bond (GVB)-procedure.³¹ This was followed by a GVB-CI calculation, which included all possible configurations arising from the various arrangements of 28 electrons in the six a_1 , five b_2 , two b_1 , and two a_2 orbitals defined above. This resulted in 42 spin eigenfunctions.

The effects of electron correlation, which are usually very important in characterizing transition states of chemical reactions, were investigated in a more elaborate configuration interaction calculation (SD-CI). These calculations were carried out for the optimized geometries of the reactants, products, and transition state obtained from the GVB-CI calculations. The starting point for the SD-CI calculations was a single-configuration Hartree–Fock (HF) calculation (Φ_1). The resulting HF orbitals were localized by using the Boys' criteria within symmetry types.³² This consistently led to a set of eight orbitals localized on the phosphine ligands and another set of six orbitals localized on the metal–hydrogen region. All single and double excitations from the latter set of orbitals into all 41 virtual orbitals were then included in the SD-CI calculations, resulting in 7227 spin eigenfunctions.

Population Analysis. A modified population analysis³³ that accounts for the diffuse nature of the metal orbitals (especially 6s and 6p) was used here. This procedure assigns electron density to metal and ligand regions on the basis of the spatial extent of basis functions in these regions. For this purpose the metal is defined as a sphere with its covalent radius. Each of the ligands is then represented by a conical section intersecting the metal sphere. In this study a covalent radius of 1.3 Å was used for the platinum.³⁴ The angle of revolution defining the hydrogen areas was chosen such that the two cones (with axes defined by the metal–hydrogen bond) were tangent.

Results

$Pt(PH_3)_2 + H_2$. The energy profile along the reaction path for addition of H_2 to $Pt(PH_3)_2$ is sketched in Figure 4 as a function

(26) Houk, K. N.; Gandour, R. W.; Strozier, R. W.; Rondan, N. G.; Paquette, L. A. *J. Am. Chem. Soc.* **1979**, *101*, 6797.

(27) Dewar, M. J. S.; Olivella, S.; Rzepa, H. S. *J. Am. Chem. Soc.* **1978**, *100*, 5650 and references therein.

(28) Noell, J. O.; Hay, P. J. *Inorg. Chem.*, **1982**, *21*, 14.

(29) Hehre, W. J.; Stewart, R. F.; Pople, J. A. *J. Chem. Phys.* **1968**, *51*, 2657.

(30) Messmer, G. G.; Anna, E. L.; Ibers, J. A. *Inorg. Chem.* **1967**, *6*, 725.

(31) Goddard, W. A., III; Dunning, T., Jr.; Hunt, W. J.; Hay, P. J. *Acc. Chem. Res.* **1973**, *6*, 368.

(32) Halgren, T. A.; Kleier, D. A.; Lipscomb, W. N. *J. Chem. Phys.* **1974**, *61*, 3905.

(33) Noell, J. O. *Inorg. Chem.* **1982**, *21*, 11.

(34) Hartley, F. R. "The Chemistry of Platinum and Palladium"; Wiley: New York, 1973; p 8.

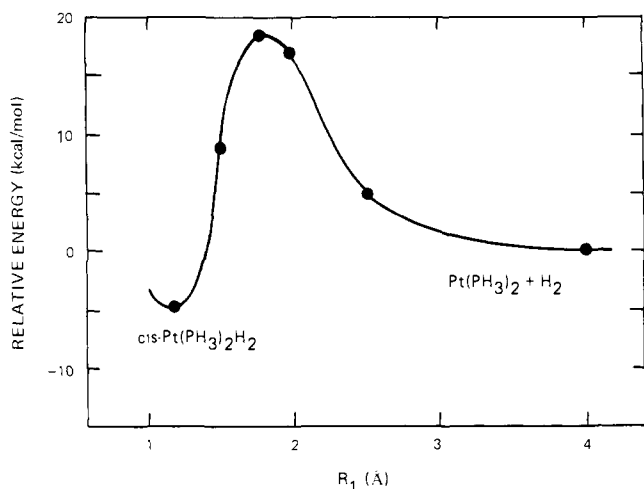


Figure 4. Energy profile of the $\text{H}_2 + \text{Pt}(\text{PH}_3)_2$ oxidative addition reaction as a function of the reaction coordinate (R_1).

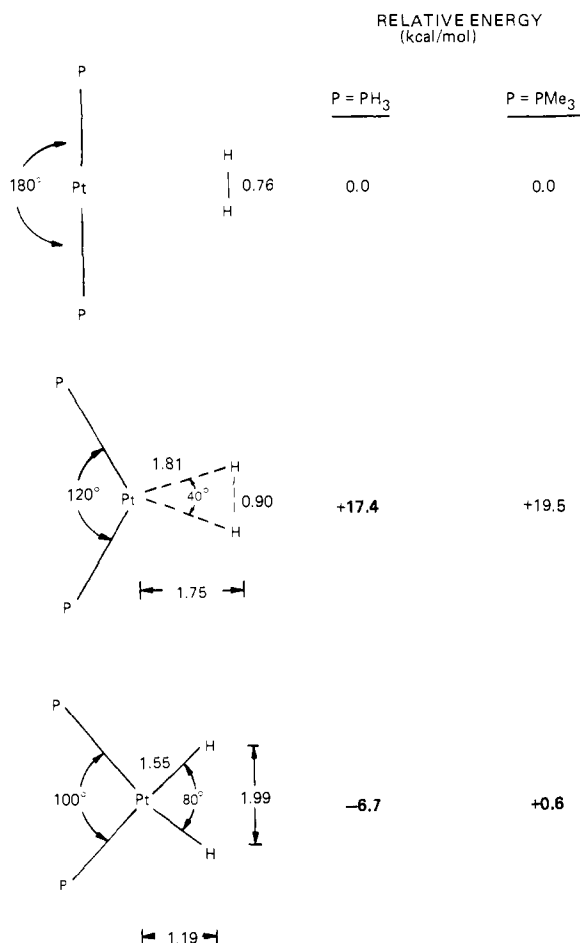


Figure 5. Geometries and relative energies of the reactants, transition states, and products for the reactions $\text{PtP}_2 + \text{H}_2$, where $\text{P} = \text{PH}_3$ and $\text{P}(\text{CH}_3)_3$.

of R_1 . An activation energy of 18 kcal/mol and an exothermicity of 5 kcal/mol are obtained from the GVB-CI calculations. In Figure 5 we compare the geometries of the reactants, transition state, and products for the reaction. (The geometries and energies along the reaction path are given in Table I.) At the transition state the Pt-H bonds are 1.81 Å, not much longer than the equilibrium bond lengths of 1.55 Å in the cis complex, the ultimate product. The H-H distance (0.9 Å), however, has not lengthened appreciably from that found in H_2 and is quite far from the 2.0-Å value attained in the product complex. Apparently then the attractive H-H interaction is preserved until the last stages of

Table I. Geometric Parameters and Relative Energies for the Oxidative Addition Reaction $\text{H}_2 + \text{Pt}(\text{PH}_3)_2 \rightarrow \text{cis-PtH}_2(\text{PH}_3)_2$ ^a

$R_1, \text{Å}$	$R_2, \text{Å}$	α, deg	relative energy, kcal/mol		
			HF ^b	GVB-CI ^c	SD-CI ^d
∞	0.76	180	0.0	0.0	0.0
4.00	0.76	180		+0.4	
2.50	0.76	167		+8.6	
2.00	0.76	140		+16.7	
1.75	0.90	120	+17.4	+18.2	+16.6
1.50	1.60	110		+8.4	
1.1874	1.9926	100	-6.7	-4.9	-5.0

^a Quantities shown refer to the reaction path obtained from GVB-CI Calculations. Also shown are relative energies from Hartree-Fock and SD-CI calculations. ^b One configuration, $E = -44.92156$ for the complex. ^c 42 configurations, $E = -44.93917$. ^d 7227 configurations, $E = -45.07399$.

Table II. Net Charge on the H and Pt Atoms Derived from Modified and Mulliken Population Analyses

$R_1, \text{Å}$	modified population analysis		Mulliken population analysis	
	q_{H}	q_{Pt}	q_{H}	q_{Pt}
1.1874	-0.29	+1.22	+0.02	-0.45
1.50	-0.20	+0.81	-0.02	-0.33
1.75	-0.11	+0.86	+0.01	-0.17
2.00	-0.02	+0.65	+0.02	-0.21
2.50	-0.01	+0.57	0.01	-0.21
4.00	-0.01	+0.53	0.00	-0.23

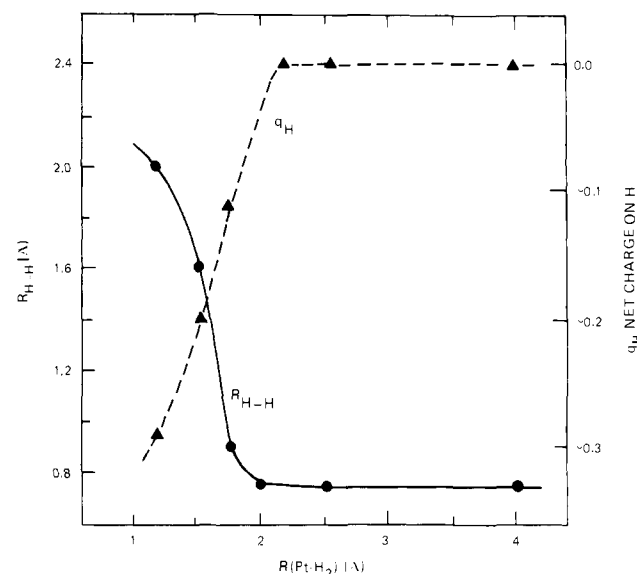


Figure 6. Variation of the H-H distance (R_2) and net charges on the H (q_{H}) as a function of the reaction coordinate (R_1).

the reaction, when metal-hydrogen bonding and anionic character set in. This surmise is supported by the results of the modified population analysis (Table II). From Figure 6 the rupture of the H-H bond, as measured by the rapid increase in $R_{\text{H-H}}$, can be seen to occur simultaneously with accumulation of negative charge on the hydrogen. Also included in Table II are the hydrogen populations calculated by the conventional Mulliken analysis. These populations differ qualitatively from the modified analysis and do not appear to reflect the chemical changes occurring in the system.)

From analysis of the charge distributions and geometrical changes, a consistent description of the process emerges. When this is viewed as an addition reaction, three phases are identifiable: (1) Initially ($R_1 \geq 0$ Å), very little happens to the hydrogen molecule, and the intruding Pt species results in only a repulsive interaction. (2) Eventually the hydrogens must become partially anionic as the $5d_{xy}$, b_2 orbital delocalizes into the hydrogen-hy-

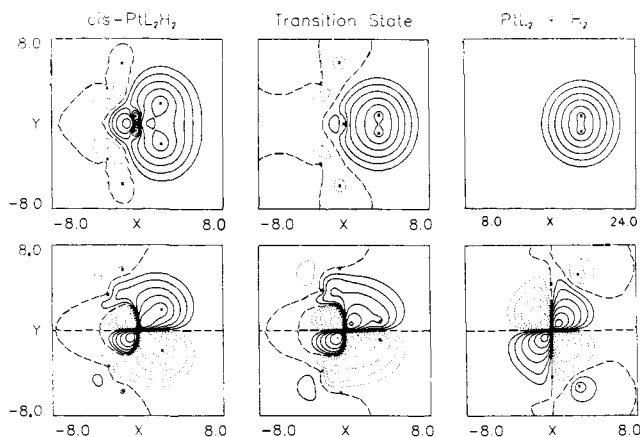


Figure 7. Contour plots of the Pt-H bonding orbitals for the reactants, transition state, and products of the $\text{H}_2 + \text{Pt}(\text{PH}_3)_2$ oxidative addition. Contours for the a_1 (upper panels) and b_2 (lower panels) localized Hartree-Fock orbitals are shown as solid (positive), dashed (negative), or long-dashed (modes) lines.

drogen antibonding orbital. (3) To alleviate this, the H-M-H angle opens very quickly, synchronous with the formation of the metal-hydrogen bonds and the development of the negative charge on the hydride ligand.

These phases of the reaction are reflected in the orbitals involved in Pt-H bond formation (Figure 7). The a_1 orbital, initially the σ_g bonding orbital of H_2 , retains its identity while incorporating some 6p and 5d components on the metal. In contrast, the b_2 orbital, initially the $5d_{xy}$ Pt orbital, shows significant delocalization onto H_2 in the transition state and more extensive metal-hydrogen charge transfer in the cis complex. The H-H antibonding component of the b_2 orbital becomes more pronounced with increased charge transfer into the H_2 σ_u orbital as the reaction proceeds.

In all of the above calculations a concerted dissociation of H_2 was assumed, with both H atoms remaining equidistant from the platinum. Two brief attempts were made to examine the possibility of a less symmetric, possibly nonconcerted, mechanism, but no evidence for a lower energy pathway was found. First an "end-on" approach of H_2 , in which a 180° Pt-H-H linkage was maintained, was examined. One can imagine this might allow charge donation from the platinum to the hydrogen without introducing as strong an antibonding H-H component, but such conformations were found to be less stable than the "side-on" configuration. For example, a collinear orientation with geometrized parameters $\angle\text{P-Pt-P} = 120^\circ$, $R(\text{Pt-H}) = 1.55 \text{ \AA}$, and $R(\text{H-H}) = 0.76 \text{ \AA}$ was found to be 20 kcal/mol above the C_{2v} transition state.

A second check for transition state of lower symmetry was performed by rotating the H_2 by 5° in the coordination plane to give unequal Pt-H bond lengths. A slight increase (<1 kcal/mol) in energy was observed. Thus no preference for an asymmetric transition state was suggested by either calculation.³⁵

Finally a comparison of the results of Hartree-Fock calculations and the considerably more extensive SD-CI calculations with the GVB-CI results in Table I reveals a surprising insensitivity of the barrier height to the effects of electron correlation, since the calculated barriers (without zero-point corrections) were 17.4, 16.6, and 18.2 kcal/mol, respectively. The slight reduction (from 7 to 5 kcal/mol) in the exothermicity in going from Hartree-Fock to a correlated wave function is also observed in the results of Table I.

$\text{Pt}[\text{Pt}(\text{CH}_3)_2]_2 + \text{H}_2$. The results of SCF calculations using the more realistic $\text{P}(\text{CH}_3)_3$ ligand in place of the PH_3 moiety, which are summarized in Figure 5 and Table III, show remarkably little difference along the reaction path leading to the *cis*- PtP_2H_2

Table III. Calculated Energies and Bond Distances for the $\text{PtP}_2 + \text{H}_2$ Reaction (from Restricted Hartree-Fock Calculations)

	P = PH_3 this work	P = $\text{P}(\text{CH}_3)_3$ this work	P = PH_3 ref 38
Relative Energy, kcal/mol			
$\text{PtP}_2 + \text{H}_2$	0.0	0.0	0.0
transition state	+17.4	+19.5	+5.2
<i>cis</i> - PtP_2H_2	-6.7	+0.6	-36.9
<i>trans</i> - PtP_2H_2	-10.6	-23.6	-38.0
Pt-H Bond Distance, \AA			
transition state	1.81	(1.81)	2.07
<i>cis</i> - PtP_2H_2	1.55	(1.55)	1.52
<i>trans</i> - PtP_2H_2	1.61	(1.61)	1.56

Table IV. Calculated and Experimental Spectroscopic Constants for the Ground State ($^2\Delta$) of PtH

PtH ($^2\Delta$ state)	Pt effective core potential		
	ref 39	calcd, this work	exptl ^a
R_e , \AA	1.47	1.51	1.528
D_e , kcal/mol	65.0	53.4	
ω_e , cm^{-1}	2260	2009	2377

^a Values for the $^2\Delta_{5/2}$ state taken from Huber and Herzberg (Huber, K. P.; Herzberg, G. "Molecular Spectra and Molecular Structure, IV. Constants of Diatomic Molecules; Van Nostrand Reinhold: New York, 1979).

complex. The transition state for the addition of H_2 to PtP_2 where $\text{P} = \text{P}(\text{CH}_3)_3$ lies 19.5 kcal/mol above the reactants, a barrier that is only 2 kcal/mol higher than the calculated barrier when $\text{P} = \text{PH}_3$. The overall exothermicity of the reaction to form *cis*- PtP_2H_2 is 7 kcal/mol smaller, however, for the case of the PMe_3 ligand (+0.6 kcal/mol) when compared to the PH_3 ligand (-6.7 kcal/mol). It is tempting to ascribe this destabilization to steric effects arising from the bulkier PMe_3 ligands since the P-Pt-P bond angle of 110° is slightly smaller than the "cone angle" of 118° estimated for this ligand.³⁶ The analogous *cis*- $\text{Pt}[\text{P}(\text{CH}_3)_2\text{Cl}]_2$ complex, however, has an even smaller bond angle of 96° , as measured by X-ray diffraction studies. These studies also noted a slight distortion of the ligands toward a tetrahedral configuration (by about 0.1 \AA out of the plane).

Our calculations also show a marked 23 kcal/mol preference for the *trans* isomer relative to *cis* for the PMe_3 complexes but relatively little preference for *trans* (4 kcal/mol) in PH_3 complexes. From the above analysis of exothermicities, at most 7 kcal/mol of this 19 kcal differential can be attributed to steric factors.

Since the energetics discussed in this section on PMe_3 ligands were obtained with the assumption of the same Pt-H bond lengths and bond angles about the Pt as in the PH_3 complexes, some caution should be taken in interpreting the results too literally. However we expect that full geometry optimizations would yield qualitatively similar conclusions.

Comparison with Other Studies. After these studies were completed, Kitaura, Obara, and Morokuma^{37,38} undertook the calculation of equilibrium geometries and transition states of the same $\text{Pt}(\text{PH}_3)_2\text{H}_2$ system to illustrate the use of the gradient technique with effective core potentials (ECP's) and to compare them with our results. Preliminary communications of their work have recently appeared, and a brief comparison of the two sets of results will be given here. Although the gradient technique afforded a full geometry optimization, the fact that Kitaura et al. employed different ECP's from the ones used here clouds the comparison between the two sets of results. In particular, since the properties of the relativistic ECP's for Pt in the two studies vary significantly, we would ascribe any difference in the results

(35) The GVB (1) solution was unstable with respect to asymmetric distortion as the reduced symmetry allowed a localization of the nearer Pt-H bond. Consequently, these comparisons were made at the RHF level. (A proper MC-SCF wave function to treat both symmetric and asymmetric geometries would involve two correlating orbitals, one for each M-H bond.)

(36) Tolman, C. A. *J. Am. Chem. Soc.* **1970**, *92*, 2956.

(37) Kitaura, K.; Obara, S.; Morokuma, K. *Chem. Phys. Lett.* **1981**, *77*, 452.

(38) Kitaura, K.; Obara, S.; Morokuma, K. *J. Am. Chem. Soc.* **1981**, *103*, 2891.

to the potentials employed than to the methods employed in optimizing geometries.

Before discussing the PtH_2 complexes, we first compare results on the PtH molecule, where one can assess directly the differences between the relativistic ECP's for Pt. As shown in Table IV, the ECP used here predicts a bond length only 0.02 Å shorter than the experimental R_e , while the ECP of Topiol and Basch³⁹ used by Kitaura et al. predicts a bond length 0.06 Å too short. The present ECP predicts the dissociation energy (D_e) of PtH to be 53 kcal/mol, which is 12 kcal/mol smaller than the D_e (65 kcal/mol) calculated with the ECP of ref 39. (While the 2-configuration GVB-1 wave functions used in each case do not include sufficient correlation effects for quantitative calculations of bond energies, the differences in calculated bond energies between different ECP's will persist, however, in more sophisticated calculations, which are capable of calculating accurate bond energies). These discrepancies between the potentials could arise from several factors: (1) We have found that overestimates of D_e can arise when spurious long-range attractive tails are present in the potentials,⁴⁰ which are scrupulously avoided in our ECP's. (2) Another important difference is the number of angular momentum symmetries appearing in the ECP, which is defined as follows:

$$V_{\text{ECP}} = V_L(r) + \sum_{l=0}^{L-1} |l\rangle \langle l| V_{l-L}(r)$$

The ECP of ref 39 contained only s, p, and d potentials ($L = 2$), while the present ECP also contains f and g contributions ($L = 4$), which are rigorously necessary to describe an atom such as Pt containing f electrons in the core. Both of these factors should lead to a more accurate description of Pt with the ECP used in this work.

This analysis of the PtH potential curves explains the differences between this study and the results of Kitaura, Obara, and Morokuma for the PtP_2H_2 complexes (Table III). Kitaura et al.^{37,38} find shorter Pt-H bond lengths (by 0.03–0.06 Å) and stronger Pt-H bond energies (by 15 kcal/mol for each Pt-H bond) in analogy with the PtH results. The barrier (5.2 kcal/mol) is 12 kcal/mol smaller than the one calculated here for cis addition of H_2 to PtP_2 . One would expect the barrier from a chemical reaction to be intimately connected with the overall thermochemistry, since one normally associates small barriers with exothermic reactions and larger barriers with thermoneutral reactions. The theoretical results are consistent with these expectations, as our potential surface has a higher barrier for a thermoneutral reaction while Kitaura et al. obtain a lower barrier for an exothermic reaction.

Discussion

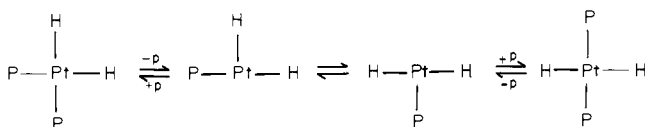
The most significant energetic result of the present calculation is the calculated barrier of 23 kcal/mol to the reductive elimination of H_2 from *cis*- $\text{PtH}_2(\text{PH}_3)_2$. This is perhaps a somewhat troubling result in that *cis* dihydride Pt(II) complexes are very infrequently observed. In an earlier paper we argued that this was not an effect of thermodynamic stability since the *trans* isomer of $\text{PtH}_2(\text{PH}_3)_2$ was found to be only 4 kcal/mol lower in energy than the *cis* isomer studied here. Yet the barrier of 23 kcal/mol is sufficiently high to ensure kinetic stability at room temperature.

There are data that suggest that the calculated barrier is not artifactual. While, to our knowledge, kinetic data for four-coordinate *cis* dihydrides do not exist, studies have been performed for the more stable six-coordinate d^6 complexes. To the extent that these two types of complexes are comparable, some inferences may be drawn from that work. One would expect similar consequences in both cases since reductive elimination from d^6 and d^8 complexes involves the same d_{xy} and H_2 σ orbitals and requires the same geometrical distortions of the ligands in the Pt-H₂ coordination plane. The d^6 complexes, however, have two additional ligands in the axial positions and formally lack an occupied d_{z^2} orbital.

The system that has been most thoroughly characterized is the addition of hydrogen to Vaska's complex, $\text{Ir}(\text{Cl})(\text{CO})(\text{PPh}_3)_2$. Chock and Halpern determined an activation barrier of 10–12 kcal/mol for this addition.⁶ When coupled with an exothermicity of 15 kcal/mol,⁴¹ this implies an activation barrier of 25 kcal/mol for the reductive elimination of hydrogen. This value, while similar to the present results, is only to be viewed as illustrative in view of the differences between Pt and Ir and between six- and four-coordinate complexes.

To resolve the nonexistence of the *cis* dihydrides (in the absence of bulky or bidentate ligands) with their calculated kinetic stability relative to reductive elimination, one is then led to consider possible pathways to the slightly thermodynamically preferred *trans* isomer. An intramolecular rearrangement of the four-coordinate species would necessarily have to pass through a quasi-tetrahedral transition state. While this possibility was not explored at length here, calculations on likely intermediates for *trans* addition revealed no pathways with barriers of less than 60 kcal/mol relative to $\text{PtP}_2 + \text{H}_2$. This possibility also appears unlikely in view of the strong preference of d^8 complexes for square-planar structures.

More likely are dissociative or associative mechanisms involving three-coordinate or five-coordinate species, respectively. The dissociative path would first yield a T-shaped intermediate, which could subsequently rearrange to the T-shaped predecessor of the *trans* isomer.



Such rearrangements have been shown to be facile for d^8 trialkyl gold(III) complexes.¹⁴

Similar pathways have been suggested³² for *cis*-*trans* isomerizations of Pt(II) complexes, but most evidence⁴³ appears to favor five-coordinate intermediates. The latter mechanism involves addition of a fifth ligand, rearrangement of the five-coordinate species, and subsequent dissociation of the fifth ligand.

The apparent greater preference for the *trans* geometry when P is a stronger σ donor, as revealed by the calculations made here using the $\text{P}(\text{CH}_3)_3$ ligand, suggests a greater thermodynamic driving force for producing *trans* dihydrides. In fact Yoshida and Otsuka¹² observed molecular addition of H_2 to PtP_2 at room temperature under normal pressure to form stable *trans* dihydride complexes for several bulky trialkylphosphines. In cases of ligands bulkier than $\text{P}(\text{CH}_3)_3$, the steric repulsions between the ligands may not be able to be accommodated in the *cis* geometries.

There are other possible explanations still extant that would explain why d^8 square-planar hydrides are only infrequently observed. The dissociation of hydrogen may not be mononuclear. Hydrogen evolution has in fact been observed⁴⁴ to proceed through a binuclear adduct for $\text{H}_2\text{Os}(\text{CO})_4$. Supporting evidence for this conjecture is the facility with which d^8 metal hydrides oligomerize with hydrogen expulsion.⁴⁵ In d^6 six-coordinate systems where metalation is not favored, the *cis* dihydride adducts are commonly observed.

Summary

The addition of H_2 to $\text{Pt}(\text{PH}_3)_2$ and $\text{Pt}[\text{P}(\text{CH}_3)_3]_2$ was examined theoretically with *ab initio* techniques. At the SCF level respective barriers of 17.4 and 19.5 kcal/mol were obtained for the two reactions. The *cis* hydride complex of PH_3 was found to be 7 kcal/mol more stable than the reactants, while the *cis* complex

(40) Hay, P. J.; Wadt, W. R.; Kahn, L. R. *J. Chem. Phys.* **1978**, *68*, 3059.

(41) Burke, N. E.; Singhal, A.; Hintz, N. J.; Ley, J. A.; Hui, H.; Smith, L. R.; Blake, D. M. *J. Am. Chem. Soc.* **1979**, *101*, 74.

(42) Kelm, H.; Louw, W. J.; Palmer, D. A. *Inorg. Chem.* **1980**, *19*, 843. Louw, W. J. *Ibid.* **1977**, *16*, 2147.

(43) Romeo, R. *Inorg. Chem.* **1978**, *17*, 2040. Romeo, R.; Miniti, D.; Trozzi, M. *Ibid.* **1976**, *15*, 1174.

(44) Evans, J.; Norton, J. R. *J. Am. Chem. Soc.* **1974**, *96*, 7577.

(45) Clark, H. C.; Goel, A. B.; Goel, S. J. *Organomet. Chem.* **1979**, *166*, C29.

(39) Basch, H.; Topiol, S. *J. Chem. Phys.* **1979**, *71*, 802.

of PMe_3 was essentially thermoneutral relative to the reactants. The trans isomer of PtP_2H_2 was 4 kcal/mol more stable than the cis form for $\text{P} = \text{PH}_3$ and 23 kcal/mol more stable for $\text{P} = \text{PMe}_3$. CI calculations on the $\text{Pt}(\text{PH}_3)_2\text{H}_2$ species showed only slight differences in the reaction barrier and reaction energy.

A C_{2v} transition state with symmetric Pt-H bonds was found, and no evidence was uncovered to support less symmetric pathways. At the transition state a significant H-H interaction is still retained, and only at later stages of the reaction does the incorporation of Pt^+-H^- character disrupt the H_2 bond. The large barrier obtained for reductive elimination of H_2 from the cis dihydride was discussed in view of the apparent instability of cis dihydride complexes.

Acknowledgment. This research was carried out under the auspices of the U.S. Department of Energy. We thank Professor

James Ibers for initially interesting us in platinum phosphine species and Professor Roald Hoffmann for an advance copy of the paper regarding the reductive elimination of metal alkyls.

Note Added in Proof. Recently Paonessa and Trogler⁴⁶ have actually observed the cis dihydrides PtP_2H_2 ($\text{P} = \text{PEt}_3$) in striking confirmation of their predicted stabilities here. These compounds, which represent the first known cis dihydrides of Pt with sterically unhindered ligands, are found to be in solvent-assisted equilibrium with the trans isomer.

Registry No. H_2 , 1333-74-0; $\text{Pt}(\text{PH}_3)_2$, 76830-85-8; $\text{Pt}[\text{P}(\text{CH}_3)_3]_2$, 82209-22-1; cis- $\text{Pt}(\text{PH}_3)_2\text{H}_2$, 76832-29-6; trans- $\text{Pt}(\text{PH}_3)_2\text{H}_2$, 76830-84-7; cis- $\text{Pt}[\text{P}(\text{CH}_3)_3]_2\text{H}_2$, 80540-35-8; trans- $\text{Pt}[\text{P}(\text{CH}_3)_3]_2\text{H}_2$, 80581-71-1.

(46) Paonessa, R. S.; Trogler, W. C. *J. Am. Chem. Soc.* **1982**, *104*, 1138.

Nature of Dilute Solutions of Sodium and Methoxide Ions in Methanol¹

William L. Jorgensen,*² Bernard Bigot,³ and Jayaraman Chandrasekhar

Contribution from the Department of Chemistry, Purdue University, West Lafayette, Lafayette, Indiana 47907. Received September 25, 1981

Abstract: Monte Carlo statistical mechanics simulations have been carried out for Na^+ and CH_3O^- in liquid methanol at 25 °C and 1 atm. The intermolecular interactions were described by Lennard-Jones and Coulomb terms in the TIPS format. Detailed information on the structures and thermodynamics of the solutions has been obtained. The computed heats and volumes of solution are in accord with available experimental data. For Na^+ in methanol, the coordination number is found to be 6, while CH_3O^- has about five solvent molecules near the oxygen. Beyond the first solvent shells the influence of the ions is much diminished. In particular, analyses of the hydrogen bonding do not show evidence for significant structure broken regions in the solutions. Rather the ions plus their first solvent shells interface readily into the bulk solvent. An interesting prediction is that the first two solvent shells around sodium ion contain the same number of methanol molecules. Although this contrasts conventional ideas about solvation, it is a consequence of the substantial compression of the first solvent shell.

I. Introduction

Much attention has been paid to the thermodynamics and structure of aqueous solutions of electrolytes because of their importance in electrochemistry and biochemistry.⁴ In comparison, nonaqueous salt solutions have received limited study;⁵ particularly little is known about their structure since diffraction experiments analogous to those for aqueous solutions have not yet been undertaken.⁶ Nevertheless, nonaqueous solutions are of paramount importance in organic chemistry since they are the principal reaction media. There is no doubt that the predictive abilities of synthetic organic chemists could be enhanced by a greater understanding of the solvation of substrates and intermediates in solution. In view of the importance of solvent effects on reactivity,^{5c,d} it is ultimately desirable to discuss reactions not largely as they are now in terms of isolated reactants, but rather with knowledge of the solvation and aggregation of the species and how

these factors vary along reaction paths. To this end, an extensive program for the theoretical study of organic chemistry in solution has been undertaken in our laboratory. The initial work has centered on Monte Carlo statistical mechanics simulations of common organic solvents including alcohols,⁷ ethers,⁸ hydrocarbons,^{9,10} and alkyl chlorides.¹⁰ An important development was the generation of a set of transferable intermolecular potential functions (TIPS) that yield good structural and thermodynamic results for these liquids.⁷⁻¹¹ In particular, the computed densities are within 0-6% of experimental values from 1 to 15 000 atm near room temperature.⁷⁻¹² Furthermore, detailed insights into the structures of the liquids have been obtained via stereoplots and numerous distributions for atomic positions, energetics, conformations, coordination numbers, and hydrogen bonding.

Now that the theoretical approach has been validated for pure liquids, attention is being turned to dilute solutions of neutral molecules and ions. An initial study described here is for sodium ion and methoxide ion in methanol. This system was chosen since

(1) Quantum and Statistical Mechanical Studies of Liquids 21.
 (2) Camille and Henry Dreyfus Foundation Teacher-Scholar, 1978-1983; Alfred P. Sloan Foundation Fellow, 1979-1981.
 (3) On leave from the Université Pierre et Marie Curie and Ecole Normale Supérieure de Saint Cloud, France; CNRS-NSF Fellow, 1980-1981.
 (4) For reviews, see: (a) "Water, A Comprehensive Treatise"; Franks, F., Ed.; Plenum Press: New York, 1973; Vol. 3. (b) Desnoyers, J. E.; Jolicœur, C. In "Modern Aspects of Electrochemistry"; Bockris, J. O'M., Conway, B. E., Eds.; Plenum Press: New York, 1969; Vol. 5, p 1.
 (5) For reviews, see: (a) Padova, J. In "Water and Aqueous Solutions"; Horne, R. A., Ed.; Wiley-Interscience: New York, 1973; p 109. (b) Garst, J. F. In "Solute-Solvent Interactions"; Coetzee, J. F., Ritchie, C. D., Eds.; Marcel Dekker: New York, 1969; p 539. (c) Abraham, M. H. *Prog. Phys. Org. Chem.* **1974**, *11*, 1. (d) Parker, A. J. *Chem. Rev.* **1969**, *69*, 1.
 (6) Neilson, G. W.; Enderby, J. E. *Annu. Rep. Prog. Chem., Sect. C* **1979**, *76*, 185.

(7) (a) Jorgensen, W. L. *J. Am. Chem. Soc.* **1981**, *103*, 341, 345. (b) Jorgensen, W. L.; Ibrahim, M. *Ibid.* **1982**, *104*, 373.
 (8) Jorgensen, W. L.; Ibrahim, M. *J. Am. Chem. Soc.* **1981**, *103*, 3976.
 (9) Jorgensen, W. L. *J. Am. Chem. Soc.* **1981**, *103*, 4721.
 (10) (a) Jorgensen, W. L. *J. Am. Chem. Soc.* **1981**, *103*, 677. (b) Jorgensen, W. L.; Binning, R. C.; Bigot, B. *Ibid.* **1981**, *103*, 4393. (c) Jorgensen, W. L.; Bigot, B. *J. Phys. Chem.*, in press.
 (11) Jorgensen, W. L. *J. Am. Chem. Soc.* **1981**, *103*, 335.
 (12) The density of liquid water at 25 °C and 1 atm has also been computed recently with the TIPS reported for water in ref 11. The computed value ($0.996 \pm 0.006 \text{ g cm}^{-3}$) is in exact agreement with experiment. Better accord for other properties of water is obtained with the TIPS2 potential (Jorgensen, W. L. *J. Chem. Phys.*, in press).